Comparison of wave characteristic due to hybrid substructures for offshore wind turbines

Min-Su Park
Structural Engineering Research Division
Korea Institute of Construction Technology
283 Goyangdae-Ro Ilsanseo-Gu Goyang-Si, Korea
mspark@kict.re.kr

Youn-Ju Jeong
Structural Engineering Research Division
Korea Institute of Construction Technology
283 Goyangdae-Ro Ilsanseo-Gu Goyang-Si, Korea
yjjeong@kict.re.kr

Young-Jun You
Structural Engineering Research Division
Korea Institute of Construction Technology
283 Goyangdae-Ro Ilsanseo-Gu Goyang-Si, Korea
yjyou@kict.re.kr

***Abstract*— For the reliable design of substructures supporting offshore wind turbines, it is very important to reduce the wave forces acting on substructures. In the present study, two hybrid substructures for offshore wind turbines are newly suggested to reduce the wave forces. The hybrid substructure (HSPG) is composed of a single pile and a gravity substructure with porous areas near free surface. The other hybrid substructure (HMPG) consists of a multi-pile near free surface and a gravity substructure at the bottom of the multi-pile. In order to calculate the wave forces acting on hybrid substructures, the fluid domain is divided into two regions and the scattering waves in each fluid region are expressed by an Eigen-function expansion method. In order to simplify the effect of porosity, Darcy's law is also applied to the porous boundary condition. The comparison of wave forces between HSPG and HMPG is made to examine the wave characteristic according to the variation of depth of interior region and pile size.**

***Keywords*— hybrid substructure, eigen-function expansion method, darcy's law, wave forces, wave run-up**

I. Introduction

Many offshore wind farms are in the planning phase. In order to construct the offshore wind farms, the substructures supporting offshore wind turbines have to resist load from wind and wave. However, the size of a substructure for wind turbines is gradually increased since the size of a tower and a rotor-nacelle becomes larger with increment of gross generation. In other words, the substructure is strongly influenced by the effect of wave forces and the safety of substructure is decreased. Therefore, it is very important to reduce the effects of wave forces for the reliable design of the substructure for wind turbines. In the present study, two hybrid substructures are newly suggested to reduce the wave forces. One is HSPG, which is composed of a single pile and a gravity substructure with a porous area near free surface since it is reported that the porous members can significantly reduce the wave force and wave run up acting on an offshore structure by many researchers [1]-[3]. The wave force can be reduced by the water wave interaction among multi-cylinders. Therefore, the other hybrid substructure is HMPG, which consists of a multi-pile near free surface and a gravity substructure at the bottom of the multi-pile. *Fig. 1* shows the conceptive design of hybrid substructures for offshore wind turbines.

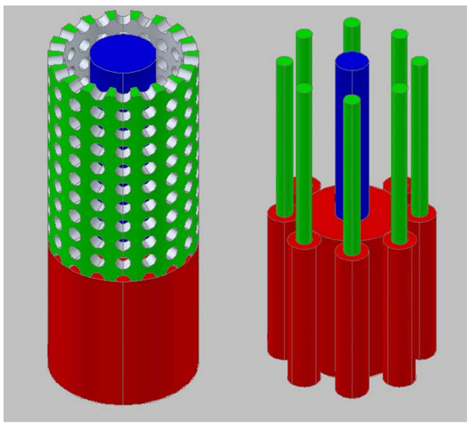

(a) HSPG (b) HMPG

Fig. 1. The conceptive design of hybrid substructures for offshore wind turbines: (a) HSPG, (b) HMPG.

In order to calculate the wave forces acting on hybrid substructures, the fluid domain is divided into two regions: an interior region and an exterior region, and the scattering waves in each fluid region are expressed by an Eigen-function expansion method with using three-dimensional linear potential theory. Using the Darcy's low, the porous boundary condition is simplified. The comparison of wave forces between HSPG

978-0-933957-40-4 ©2013 MTS

and HMPG is made to examine the wave characteristic according to the variation of depth of interior region and pile size. Moreover, the water wave interaction with multi-pile is presented.

II. FORMULATION

An arbitrary array of N hybrid substructures is situated in water of uniform depth d and the draughts of each permeable and impermeable area of hybrid substructure are h and c, respectively. The outer and the inner radius of the jth hybrid substructure are a_j and b_j, respectively. Also, the global cartesian coordinate system(x, y, z) is defined with an origin located on the sea bed with the z-axis directed vertically upwards. The center of each hybrid substructure at (x_j, y_j) is taken as the origin of a local polar coordinate system (r_j, θ_j), where θ_j is measured counter- clockwise from the positive x-axis. The center of the lth hybrid substructure has a polar coordinate (R_{jl}, α_{jl}) relative to the jth hybrid substructure. The coordinate relationship between the jth and lth hybrid substructure is shown in *Fig. 2*. Moreover, the fluid domain is divided into two regions: region 1 which is interior to the hybrid substructure ($b_j \le r_j \le a_j$, $d-h \le z \le d$), and region 2 which is exterior to the hybrid substructure and extends to infinity in the horizontal plane ($a_j \le r_j$, $0 \le z \le d$).

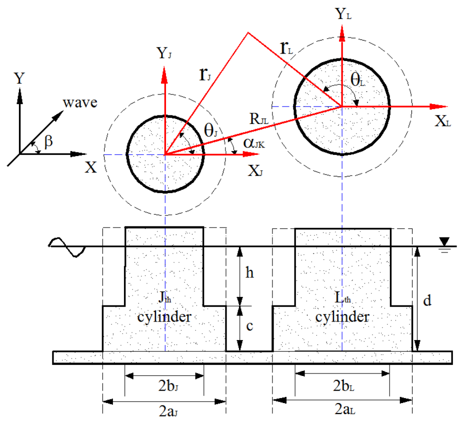

Fig. 2. Coordinate system for an array of offshore substructures.

It is assumed that the computational fluid domain is inviscid, and incompressible, and its motion is irrotational. The array of hybrid substructures is subjected to a train of regular waves of height H and wave frequency ω propagating at an angle β to the positive x-axis. The wave potential in the interior region of the jth hybrid substructure can be expressed by the following Eigen-function expansion,

$$\phi_1^j = \sum_{n=-\infty}^{n=\infty}\left[A_n^j J_n\left(k_0 r_j\right) - \frac{J_n'\left(k_0 b_j\right)}{Y_n'\left(k_0 b_j\right)} A_n^j Y_n\left(k_0 r_j\right)\right] \times \frac{\cosh\{k_0(z-d+h)\}}{\cosh(k_0 h)} e^{in\theta_j} \quad (1)$$

in which J_n and Y_n denotes the Bessel function of the first and the second kind of order n, respectively. A_n^j is the unknown complex potential coefficient. A new wave number k_0 is introduced, which satisfies the dispersion relation $\omega^2 = gk_0 \tanh k_0 h$, where g and h denote the gravitational acceleration and the local water depth in the interior region 1, respectively.

The wave potential in the exterior region 2 can be expressed by the following Eigen-function expansion [4],

$$\phi_2^j(r_j,\theta_j) = \sum_{n=-\infty}^{n=\infty}\left[\begin{array}{l} e^{ik(x_j\cos\beta + y_j\sin\beta)} J_n\left(kr_j\right) e^{in(\pi/2-\beta)} + C_n^j \dfrac{H_n\left(kr_j\right)}{H_n'\left(ka_j\right)} \\ + \displaystyle\sum_{\substack{l=1 \\ l\neq j}}^{N} \sum_{m=-\infty}^{m=\infty} C_m^l \dfrac{J_n\left(kr_j\right)}{H_m'\left(ka_j\right)} H_{m-n}\left(kR_{lj}\right) e^{i(m-n)\alpha_{lj}} \end{array}\right] \times \frac{\cosh kz}{\cosh kd} e^{in\theta_j} \quad (2)$$

k is the incident wave number which is related to the wave frequency through the dispersion relation, $\omega^2 = gk \tanh kd$, with the water depth d. The right-hand side of (2) represents the incident wave upon the jth substructure, the scattered wave produced by the jth substructure, and the re-scattered wave generated by the adjacent substructure l, respectively. C_n^j is the unknown complex potential coefficient. H_n is the Hankel function of first kind of order n, and J_n' and H_n' are the first derivatives of the Bessel and Hankel function of the first kind, respectively.

In addition to the boundary conditions, the fluid flow passing through the porous surface of hybrid substructure is assumed to obey Darcy's law. Therefore it can be written as follows [2],

$$\frac{\partial \phi_1^{(j)}}{\partial r} = \frac{\gamma}{\mu}\rho i\omega\left[\phi_1^{(j)} - \phi_2^{(j)}\right] \quad on \quad r_j = a_j \quad j = 1,2,3,\dots,N \quad (3)$$

where μ is the coefficient of dynamic viscosity, γ is a material constant having the dimension of length and ρ is the fluid density, respectively. Subsequently, the porosity of the hybrid substructure will be characterized by the dimensionless parameter, G. The body boundary condition on the porous surface of hybrid substructure can be expressed with the G.

$$\frac{\partial \phi_1^{(j)}}{\partial r} = ik_0 G\left[\phi_1^{(j)} - \phi_2^{(j)}\right] \quad , Here \quad G = \frac{\rho\omega\gamma}{\mu k_0} \quad (4)$$

Applying matching conditions and exploiting the orthogonality of depth, the key equation for unknown coefficients C_n^j can be obtained as follows,

$$\begin{aligned} & C_n^j\left\{kS_1 - \frac{Q_1 k_0 S_2}{Q_3 S_3}\frac{H_n\left(ka_j\right)}{H_n'\left(ka_j\right)} H_n(ka)\frac{S_2}{S_3}\right\} \\ & + \sum_{\substack{l=1 \\ l=j}}^{N}\sum_{m=-M}^{m=M} C_m^l \frac{H_{m-n}\left(kR_{lj}\right)}{H_m'\left(ka_l\right)} e^{i(m-n)\alpha_{lj}} \left\{\begin{array}{l} J_n'\left(ka_j\right)kS_1 \\ -\dfrac{Q_1 k_0 S_2}{Q_3 S_3} J_n\left(ka_j\right)\end{array}\right\} \\ & = -e^{ik(x_j\cos\beta + y_j\sin\beta)} e^{in(\pi/2-\beta)}\left\{J_n'\left(ka_j\right)kS_1 - \frac{Q_1 k_0 S_2}{Q_3 S_3} J_n\left(ka_j\right)\right\} \end{aligned} \quad (5)$$

$$S_1 = \int_0^d \left\{ \frac{\cosh kz}{\cosh kd} \right\}^2 dz$$

where, $$S_2 = \int_{d-h}^{d} \left\{ \frac{\cosh k_0 (z-d+h)}{\cosh k_0 h} \frac{\cosh kz}{\cosh kd} \right\} dz \times \int_{d-h}^{d} \left\{ \frac{\cosh k_0 (z-d+h)}{\cosh k_0 h} \frac{\cosh kz}{\cosh kd} \right\} dz$$

$$S_3 = \int_{d-h}^{d} \left\{ \frac{\cosh k_0 (z-d+h)}{\cosh k_0 h} \right\}^2 dz$$

$$Q_1 = \left\{ J_n'(k_0 a_j) - \frac{J_n'(k_0 b_j)}{Y_n'(k_0 b_j)} Y_n'(k_0 a_j) \right\}$$

$$Q_2 = \left\{ J_n(k_0 a_j) - \frac{J_n'(k_0 b_j)}{Y_n'(k_0 b_j)} Y_n(k_0 a_j) \right\}, \; Q_3 = Q_2 + \frac{i}{G} Q_1$$

By using a stand matrix technique, the equations on C_n^j can be solved and the unknown coefficients A_n^j may then be obtain from (4) by applying C_n^j. In this manner the velocity potential in each fluid region (ϕ_1^j, ϕ_2^j) can be determined. After solving the velocity potentials, the wave forces on each hybrid substructure are obtained using the integration of pressure on the wetted surface of substructure. Wave forces in x-direction (F_x) and in y-direction (F_y) are calculated as follows,

$$F_x^j = -i\rho\omega \int_{d-h}^{d} \int_0^{2\pi} \frac{-igH}{2\omega} \left\{ \phi_2^j - \phi_1^j \right\} a_j \cos\theta d\theta dz \; on \; d-h \le z \le d$$
$$F_y^j = -i\rho\omega \int_{d-h}^{d} \int_0^{2\pi} \frac{-igH}{2\omega} \left\{ \phi_2^j - \phi_1^j \right\} a_j \sin\theta d\theta dz \; on \; d-h \le z \le d \tag{6}$$
$$F_x^j = -i\rho\omega \int_{d-h}^{d} \int_0^{2\pi} \frac{-igH}{2\omega} \left\{ \phi_1^j \right\} b_j \cos\theta d\theta dz \; on \; d-h \le z \le d$$
$$F_y^j = -i\rho\omega \int_{d-h}^{d} \int_0^{2\pi} \frac{-igH}{2\omega} \left\{ \phi_1^j \right\} b_j \sin\theta d\theta dz \; on \; d-h \le z \le d$$
$$F_x^j = -i\rho\omega \int_0^{d-h} \int_0^{2\pi} \frac{-igH}{2\omega} \left\{ \phi_2^j \right\} a_j \cos\theta d\theta dz \; on \; 0 \le z \le d-h \tag{7}$$
$$F_y^j = -i\rho\omega \int_0^{d-h} \int_0^{2\pi} \frac{-igH}{2\omega} \left\{ \phi_2^j \right\} a_j \sin\theta d\theta dz \; on \; 0 \le z \le d-h$$

where (6) is for porous areas and (7) is for impermeable areas of hybrid substructure.

III. Numerical and Discussion

In order to verify the accuracy of the calculated wave forces on an array of four hybrid substructures (HSPG), the present numerical results are compared with the numerical results of Sankarbabu [5]. *Fig. 3* shows the comparison of wave forces on the array of four hybrid substructures for various depths (*h/d*) of interior region. The calculation conditions are *a=10.0m*, *b/a=0.5*, *d/a=5*, *G=1.0* and $\beta=0.0^0$. The hybrid substructures are numbered clockwise from *1* to *4*, and situated at *(-30.0, 30.0)m*, *(30.0, 30.0)m*, *(30.0, -30.0)m*, and *(-30.0, -30.0)m*, respectively. The distance between cylinder centers (*S*) is *60.0m*, which is 6 times of cylinder radius (*S/a=6*). In the comparison the ratio of *h/d=0.0* indicates the full-body impermeable hybrid substructure, while *h/d=1.0* represents the full-body porous hybrid substructure. The calculated outer and total wave forces are normalized by $\rho g(H/2)a^2$ and the inner wave forces by $\rho g(H/2)b^2$.

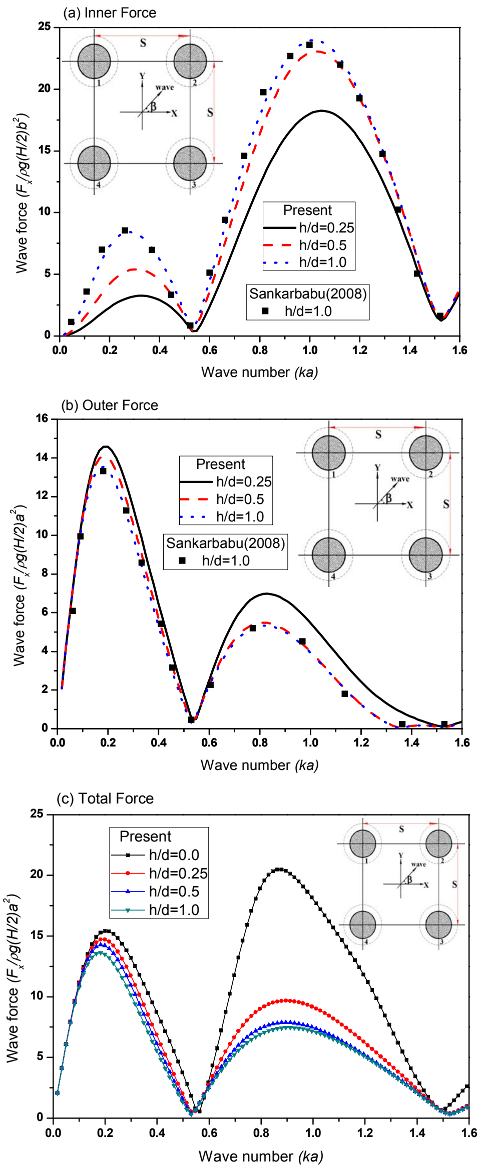

Fig. 3. Dimensionless wave forces on the group of four hybrid substructures (HSPG) with *b/a=0.5, d/a=4, h/d=0.5, G=1.0,* $\beta=0^0$ for various depths of interior region: (a) Inner force, (b) Outer force, (c) Total force.

The inner wave force is increased since the amount of incident wave passing through porous area is increased as the depth of interior region increases. Although in the long wave region ($ka \le 0.55$) the pattern of inner wave force is strongly influenced by the depth, the pattern of both depth 0.5 and 1.0 becomes very similar in the short wave region ($ka \ge 0.55$). The outer wave force is inversely decreased with increment of depth compared to the case of inner wave force. The difference of outer wave force between the depth 0.5 and 1.0 is also very small in the short wave region ($ka \ge 0.55$). The comparison of total surge force between the hybrid substructure (HSPG) and the full-body impermeable gravity substructure is made in *Fig. 3(c)*. In the comparison, the total wave forces of hybrid substructure with depth 0.5 at the first and second peaks (at $ka=0.19$ and $ka=0.86$) decrease about *8.0%* and *62.0%*, respectively, compared to full-body impermeable substructure. Especially, the hybrid substructure (HSPG) is significantly effective to reduce the effect of wave force in the short wave region. Moreover the calculated wave forces are in good agreement with the results from Sankarbabu [5] in the case of full-body impermeable hybrid substructure.

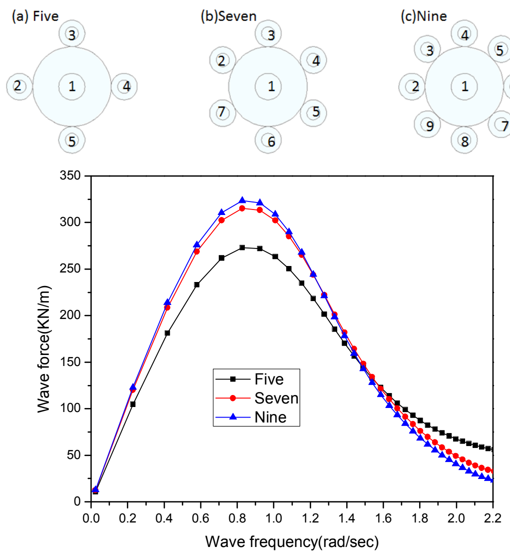

Fig. 4. Comparison of total wave forces on the hybrid substructure(HMPG) of various cylinder numbers with a_1=3.0m, b_1=1.0m, a_j=1.0m, b_j=0.5m(j=2,3,…,7) and $d=20.0m$ for various incident wave angles (β).

The Comparison of total wave forces on the hybrid substructure (HMPG) with various cylinder numbers is presented in *Fig. 4* to examine the water wave interaction among cylinders. The calculation conditions are $a_1=3.0m$, $b_1=1.0m$, $a_j=1.0m$, $b_j=0.5m$ $(j=2,3,\ldots,9)$ and $d=20.0m$. The depth (h/d) of interior region is 0.5, the largest cylinder 1 is located at center, and the other cylinders are numbered clockwise from 2 to 9 shown in *Fig 4*. In the long wave region ($\omega\leq 1.5$) the peak wave force of nine cylinders is largest and the difference of peak between seven cylinders and nine cylinders is small. The wave forces of nine cylinder gradually decreases and especially has a lower value than those of five cylinders in the short wave region($\omega\geq 1.5$). The difference between five cylinder and nine cylinders becomes larger when the wave frequency becomes greater than 1.5. It means that wave forces are strong influenced by the wave length, and the water wave interaction is strongly depended on the relation between the wave length and the number of cylinders. Moreover, the hybrid substructure (HMPG) is significantly efficient to reduce the wave forces in the short wave region.

Fig. 5 shows the comparison of wave forces between HSPG and HMPG for various depths (h/d) of interior region. The calculation conditions of HMPG are $a_1=3.0m$, $b_1=1.0m$, $a_j=1.0m$, $b_j=0.5m$ $(j=2,3,\ldots,9)$ and $d=20.0m$. HSPG is $a=4.0m$, $b=1.5m$, $G=1.0$ and $d=20.0m$. In case of HSPG, the wave forces decrease as the depth of interior region increases. The difference of wave force between the depth 0.5 and 0.75 is also very small in the short wave region. It means that the hybrid substructure (HSPG) with depth 0.5 is very efficient to reduce the effect of wave force in the short wave region. In case of HMPG, the peak wave force with depth 0.5 and 0.75 decreases about 28% and 48%, respectively, compared to the peak value of depth 0.25. Although in the long wave region the pattern of wave forces is strongly influenced by the depth of interior region, the pattern of both depth 0.5 and 0.75 becomes very similar. The difference between depth 0.5 and 0.75 is also very small in the short wave region. The wave forces on the hybrid substructure are remarkably smaller than those on mono pile. It means that the suggested hybrid substructure with depth of interior region 0.5 is significantly efficient to reduce the wave forces in the short wave region.

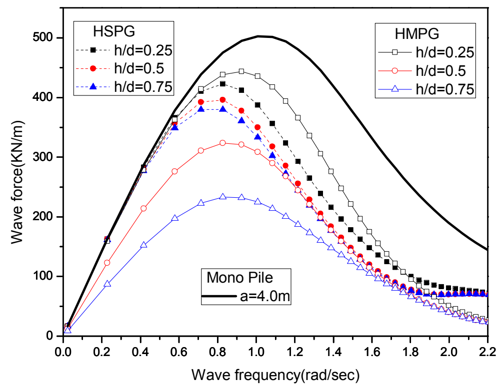

Fig. 5. Comparison of total wave forces on the hybrid substructure with $d=20.0m$ and $\beta=0.0^0$ for various depths (h): HSPG($a=4.0m$, $b=1.5m$, $G=1.0$) and HMPG($a_1=3.0m$, $b_1=1.0m$, $a_j=1.0m$, $b_j=0.5m$ $(j=2,3,..,9)$.

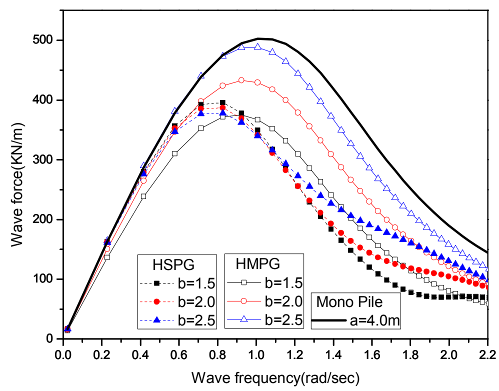

Fig. 6. Comparison of total wave forces on the hybrid substructure with $h/d=0.5$, $d=20.0m$ and $\beta=0.0^0$ for various radiuses (b_1): HSPG($a=4.0m$, $G=1.0$) and HMPG($a_1=3.0m$, $a_j=1.0m$, $b_j=0.5m$ $(j=2,3,..,9)$.

Fig. 6 shows the comparison of total wave forces on the hybrid substructure for various radiuses (b_1). Since the wave force is closely related to the wetted surface of structure, the wave forces gradually increase with the increment of radius in case of HMPG. Although the wave force of HSPG increases as the radius becomes larger in the short wave region, it has a very similar value in the long wave region. The hybrid substructure with the radius of interior region less than 1.5 is remarkably efficient to reduce the wave forces.

IV. CONCLUSION

Two hybrid substructures (HSPG, HMPG) are newly suggested to reduce the effect of wave force acting on substructures for wind turbines. The 3D numerical method for hybrid substructures is developed using the Eigenfunction expansion method and Darcy's law under the linear potential theory. For verification of the present method, the calculated results for an array of four hybrid substructures (HSPG) are compared. It is found that the present method has so accurate. In the short wave region, the suggested hybrid substructure with depth of interior region 0.5 is significantly efficient to reduce the wave forces compared to a mono pile. Moreover the hybrid substructure with the radius of interior region less than 1.5 remarkably reduces the wave forces. Consequently, the suggested hybrid substructure for wind turbines can be an effective substructure for reducing hydrodynamic effects.

ACKNOWLEDGMENT

This study was supported by the Korea Institute of Energy Technology Evaluation and Planning through the research project "Development of hybrid substructure systems for offshore wind power" (2011T100200105).

REFERENCES

[1] M. Park, W Koo, Y. Choi, "Hydrodynamic interaction with an array of porous circular cylinders," International Journal of Naval Architecture and Ocean Engineering, 2010, 2(3), pp. 146-154.

[2] A. Williams, W. Li, "Water wave interaction with an array of bottom-mounted surface-piercing porous cylinder," Ocean Engineering, 2000, 27, pp. 841-866.

[3] F. Zhao, W. Bao, T. Kinoshita, H. Itakura, "Theoretical and experimental study on a porous cylinder floating in waves," Journal of Offshore Mechanics and Arctic Engineering, 2011, 133, pp. 301-311.

[4] M. Abramowitz, I. Stegun, Handbook of Mathematical Functions. Dover Publications, New York, 1972.

[5] K. Sankarbabu, S. Sannasiraj, V. Sundar, "Hydrodynamic Performance of a Dual Cylindrical Caisson Breakwater," Coastal Engineering, 2008, 55, pp. 431-446.